

Quasiparticle Trapping at Vortices Producing Josephson Supercurrent Enhancement

Yosuke Sato^{1,2,*}, Kento Ueda^{1,†}, Yuusuke Takeshige¹, Hiroshi Kamata³, Kan Li⁴,
Lars Samuelson^{5,6}, H. Q. Xu^{4,5,7,‡}, Sadashige Matsuo^{2,8,§}, and Seigo Tarucha^{2,9,||}

¹*Department of Applied Physics, University of Tokyo, 7-3-1 Hongo, Bunkyo-ku, Tokyo 113-8656, Japan*

²*Center for Emergent Matter Science, RIKEN, 2-1 Hirosawa, Wako-shi, Saitama 351-0198, Japan*

³*Laboratoire de Physique de l'École Normale Supérieure, ENS, PSL Research University, CNRS, Sorbonne Université, Université Paris Diderot, Sorbonne Paris Cité, 24 rue Lhomond, 75231 Paris Cedex 05, France*

⁴*Beijing Key Laboratory of Quantum Devices, Key Laboratory for the Physics and Chemistry of Nanodevices and School of Electronics, Peking University, Beijing 100871, China*

⁵*Division of Solid State Physics and NanoLund, Lund University, Box 118, SE-221 00 Lund, Sweden*

⁶*Department of Electrical and Electronic Engineering, Southern University of Science and Technology, 1088 Xueyuan Blvd, Nanshan, Shenzhen, Guangdong 518055, China*

⁷*Beijing Academy of Quantum Information Sciences, Beijing 100193, China*

⁸*JST, PRESTO, 4-1-8 Honcho, Kawaguchi, Saitama 332-0012, Japan*

⁹*RIKEN Center for Quantum Computing, RIKEN, 2-1 Hirosawa, Wako-shi, Saitama 351-0198, Japan*



(Received 24 November 2021; accepted 4 April 2022; published 19 May 2022)

The Josephson junction of a strong spin-orbit material under a magnetic field is a promising Majorana fermion candidate. Supercurrent enhancement by a magnetic field has been observed in the InAs nanowire Josephson junctions and assigned to a topological transition. In this work we observe a similar phenomenon but discuss the nontopological origin by considering the trapping of quasiparticles by vortices that penetrate the superconductor under a finite magnetic field. This assignment is supported by the observed hysteresis of the switching current when sweeping up and down the magnetic field. Our experiment shows the importance of quasiparticles in superconducting devices with a magnetic field, which can provide important insights for the design of qubits using superconductors.

DOI: [10.1103/PhysRevLett.128.207001](https://doi.org/10.1103/PhysRevLett.128.207001)

Introduction.—Combining an *s*-wave superconductor with a semiconductor nanowire (NW) made of strong spin-orbit interaction (SOI) materials, such as InAs and InSb, is of experimental interest, because it induces a topological transition to the topological superconductor (TSC) phase with suitable magnetic fields and chemical potential [1,2]. The TSC phase of the NW coupled to the superconductor has Majorana fermions (MFs) at the edge. The MFs are expected to be applied to topologically protected quantum computing because of their non-Abelian statistics, and recently, research on superconductor-semiconductor NW hybrid systems has been developed to find and control the MFs [3,4]. In the literature, the zero-bias conductance peak [5–9], missing odd Shapiro steps [10], Josephson emission at half of the fundamental radiation frequency [11], and the enhancement of supercurrent (SC) [12] have been presented as experimental evidence of MFs or TSC phase. In these studies, the magnetic field is a crucial parameter that induces nontrivial topological states. However, there have been criticisms of the experimental evidence. Critics argue that the observed phenomena can arise from a trivial source unrelated to the MFs. For example, the zero-bias conductance peak can be

attributed to the Andreev bound state (ABS) [13–17] or weak antilocalization [18]. In addition, the missing odd-integer Shapiro steps can be explained by nonadiabatic dynamics such as the Landau-Zener transition of the highly transparent Josephson junctions [19–21]. These recent criticisms indicate that thorough experimental study and careful data analysis to identify the origin of the novel superconducting transport phenomena are of great importance—significantly, for the establishment of not only TSC and MF physics, but also the development of superconducting device physics.

In this Letter, we focus on the magnetic-field-induced enhancement of SC in the Josephson junction of a single InAs NW [12]. This enhancement shows that the switching current almost doubles above a certain magnetic field B^* as the positive out-of-plane magnetic field is swept from 0 mT. In the first place, this previous report discusses that the most critical contribution to the enhancement is topological transition of the proximitized region under the superconducting electrodes, followed by the MF emergence as suggested theoretically [23]. In contrast, we have previously reported a similar experimental study [22] on the Josephson junction of an InAs single NW, where we found

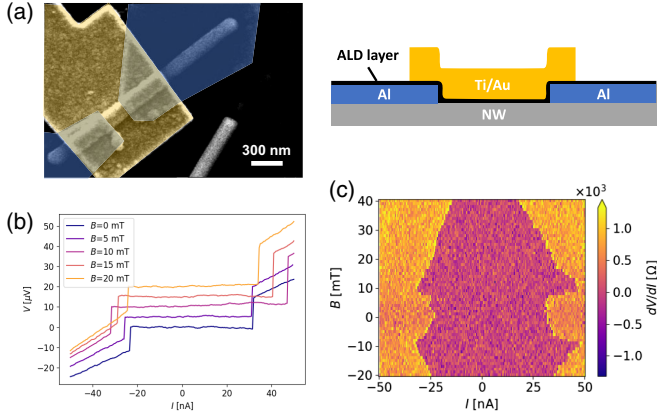


FIG. 1. (a) Left: SEM image of an InAs single NW Josephson junction device with a top gate electrode (yellow). The junction separation between the two Al (blue) electrodes was approximately 200 nm. The NW looks thicker than 80 nm because of the Al_2O_3 layer. Right: Schematic view of cross section along NW. (b) Examples of V vs I measured for various magnetic fields. Each curve was offset by $5 \mu\text{V}$. (c) dV/dI as a function of I and B . I_{sw} had a maximum at $B = 10 \text{ mT}$.

an enhancement of SC for the in-plane parallel magnetic field in the NW direction. We concluded that this enhancement can be interpreted as low-pass filter formation, which is not related to the MFs and TSC. However, in this experimental report, we did not study the out-of-plane SC enhancement which is the most remarkable in the previous report [12]. Therefore, it is valuable to revisit the SC enhancement with the out-of-plane magnetic field.

For this purpose, we fabricated a Josephson junction on an epitaxially grown InAs single NW and performed a DC measurement of the SC in a dilution refrigerator. Consequently, we observed the enhancement of the SC, as reported in a previous study [12,22]. To determine the origin of the enhancement, we measured the switching current evolution with the gate voltage and magnetic field. Then, we found that B^* does not depend on the gate voltage, the B^* is determined only by the out-of-plane magnetic field component, and the magnetic field dependence shows a clear hysteresis with respect to the magnetic field sweep direction. These results suggest that the magnetic-field-induced SC enhancement is related to the vortices penetrating the superconducting electrodes. Thus, we assign the enhancement origin to quasiparticles trapped in the vortex cores. Our results will contribute to the physics of superconducting devices and especially sort anomalous superconducting transport phenomena into trivial and nontrivial topological natures.

Results.—In this study, a Josephson junction is fabricated on an InAs single NW placed on a Si substrate. A scanning electron microscopy (SEM) image of the complete device and a schematic picture of the cross section along the NW are shown in Fig. 1(a). We use two superconductor Al electrodes that are separated by approximately 200 nm.

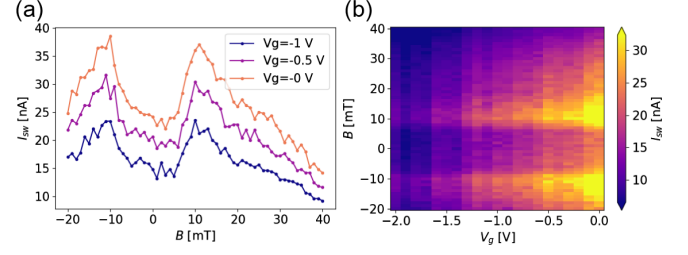


FIG. 2. (a) I_{sw} as a function of B at different V_g . (b) I_{sw} as a function of B and V_g . B^* is found to be independent of V_g .

The carrier density of the NW is controlled using a top gate electrode. The voltage V across the junction as a function of the current I measured under various magnetic fields for a bath temperature of $T = 37 \text{ mK}$ is shown in Fig. 1(b). Figure 1(c) shows the differential resistance dV/dI as a function of the bias current I and out-of-plane magnetic field B for the device at $V_g = 0 \text{ V}$. We note that the Josephson junction fabricated with the same process typically indicates high transmission ($0.7 \sim 0.9$) [24].

The boundary identified by the color change gives the magnitude of the SC and switching current I_{sw} . The I_{sw} at $B = 0 \text{ mT}$ is 30 nA and gradually increases as B increases to 10 mT, where it reaches a maximum. We denote this maximum point as B^* . I_{sw} then decreases and vanishes at $B = 60 \text{ mT}$. This result is similar to the previous report [12], including in terms of the magnitude of the enhancement. It should be noted that dV/dI in the SC region remains zero at all measured B . This is a significant difference from the in-plane magnetic field case in Ref. [22], because the enhancement with the in-plane field is derived from a partial breakdown of superconductivity due to difference in thickness, which ends up as the formation of low-pass filters, causing the finite dV/dI at $|B| > |B^*|$.

To investigate whether the enhancement originated from the NW, the proximitized regions, or superconducting metals, we vary the electron density of the NW by V_g . Figures 2(a) and 2(b) show I_{sw} as a function of B and V_g . Note that the junction can be completely depleted at $V_g = -5.1 \text{ V}$ (See Sec. 1 of the Supplemental Material [25]). The B^* remains constant, whereas I_{sw} changes when varying the electron density of the NW with V_g . This result indicates that the enhancement does not originate from the NW between the two superconducting electrodes, but from the superconducting metals or the proximitized NW regions beneath the superconducting metals.

We study dV/dI dependence on I and B by changing the direction of the magnetic field, as shown in Fig. 3(a). The magnetic field is applied at an out-of-plane angle ϕ measured from the plane. We observe an increase in the B^* as the applied B tilts from the out-of-plane ($\phi = 90^\circ$) to the in-plane ($\phi = 0^\circ$) direction. In Fig. 3(a), the enhancement peak points B^* are highlighted with blue circles.

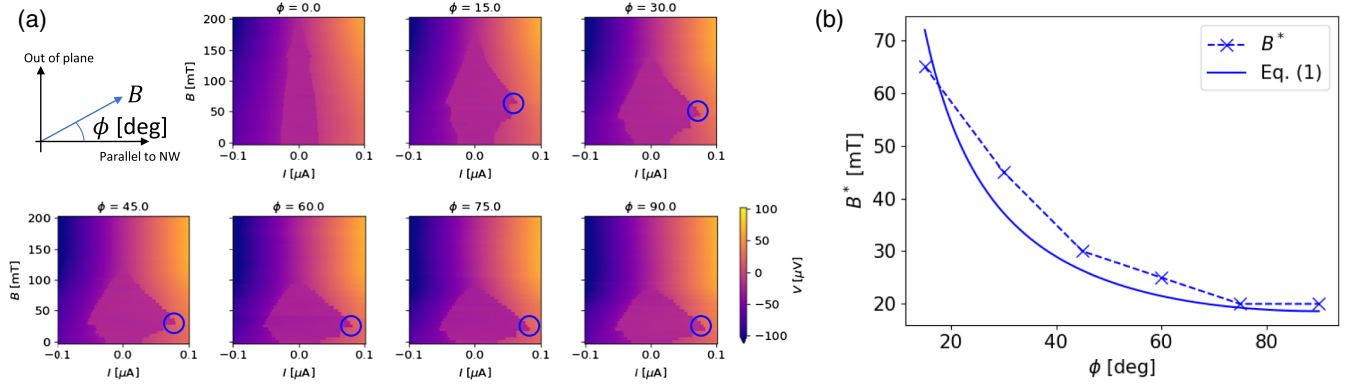


FIG. 3. (a) Bias voltage V as a function of B and I . The blue circles indicate B^* . (b) Magnetic field B^* vs ϕ (blue crosses). The blue solid line is the fitting result of the B^* vs ϕ data points to Eq. (1). The fitting parameter is given as $A = 18.6 \pm 1.1$ mT.

Here, we fit B^* [the crosses in Fig. 3(b)] as a function of the angle ϕ using the following formula:

$$B^* = \frac{A}{\sin \phi}, \quad (1)$$

where A corresponds to the out-of-plane component of B^* . The solid line in Fig. 3(b) shows the calculated magnetic field of Eq. (1) compared to the experimentally obtained B^* . The good agreement with the experiment indicates that only the out-of-plane magnetic field component determines B^* .

Finally, we investigate the B dependence of I_{sw} when B is swept in different directions. Figures 4(a)–4(c) show I_{sw} as a function of B at $T = 37$ mK, 375 mK, and 425 mK, respectively. The blue (purple) lines represent the upward (downward) sweep. Here, we find a clear hysteresis of I_{sw} depending on the B sweep direction, as shown in Fig. 4. The hysteresis is apparent for $|B| < |B^*|$, while it does not appear for $|B| > |B^*|$. Furthermore, in Fig. 4(a), I_{sw} in $-B^* < B < 0$ mT is larger than that in $0 < B < B^*$ in the sweep from negative to positive and vice versa. In Figs. 4(b) and 4(c), the hysteresis appears between $\pm B^*$ and dips around ± 5 mT and has the same sweep-direction dependence. Note that the out-of-plane B dependence of I_{sw} in Ref. [12] is also asymmetric for $B^* > B > 0$ mT and $-B^* < B < 0$ mT, suggesting hysteresis. Also, note that supercurrent enhancement has been observed in similar nanowire systems [23,28], but these results do not show

hysteresis of B field sweep, meaning the origins of the enhancement are different from ours.

Discussion.—We attribute the observed enhancement to quasiparticle trapping by superconducting vortices. The vortices penetrate a superconductor when a magnetic field applied to the superconductor exceeds the critical field B_{c1} . The superconducting pair potential is broken at the vortex cores, and they act as trapping potentials for quasiparticles. These quasiparticles correspond to the excited states in the superconductors. Therefore, trapping at the vortex cores makes the thermally excited quasiparticles relax to the bound states in the cores whose energies are lower. In the relaxation process, the thermally excited states transfer their energies to the environment (heat bath) as phonons (see Sec. 4 of the Supplemental Material [25]). This type of quasiparticle trapping can improve the superconducting device quality, as observed in electron turnstile devices [29–31], because the trapping effectively lowers the electron temperature. This effect has been applied to the design of superconducting qubits—for example, forming vortices in the outer region so that the system of interest is cooled down [32–35]. The switching current I_{sw} is affected by thermally excited quasiparticles, depending on the electron temperature [36]. Therefore, the observed SC enhancement can be attributed to electron cooling due to quasiparticle trapping.

In this scenario, the observed hysteresis is also reasonable. B^* is the point that vortices enter the system, and they

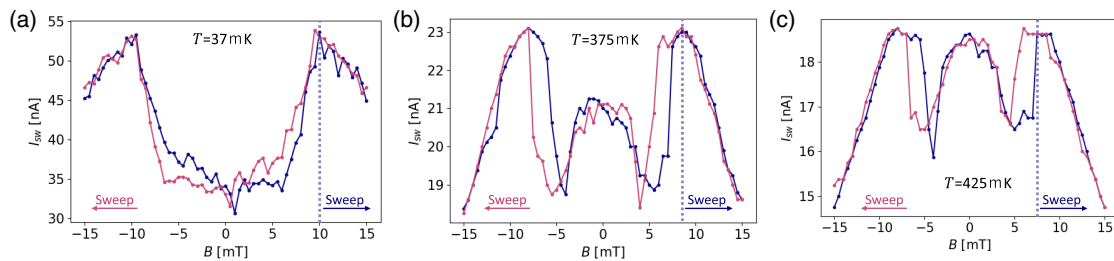


FIG. 4. I_{sw} vs B at (a) $T = 37$ mK, (b) 375 mK, (c) and 425 mK. The blue (purple) lines represent the results for the upward (downward) sweep. The hysteresis is visible for $|B| < |B^*|$. B^* determined in the upward sweep is shown as dashed lines.

always exist at $|B| > |B^*|$. The hysteresis appears, for example, when we sweep downward from $B > B^*$. Here, some magnetic fluxes remain in the system due to the pinning effect by impurities or diffraction and provide the cooling effect. This is consistent with the result that the I_{sw} of a downward sweep is larger than that of an upward sweep where $0 < B < B^*$. When comparing the results at several temperatures in Fig. 4, it is observed that B^* (dashed lines) decreases with increasing T . This indicates that B_{c1} becomes smaller as T increases, supporting the electron cooling scenario.

In addition, the enhancement at $B = B^*$ gradually decreases as T increases. This behavior is consistent with the decrease in the electron cooling effect at higher temperatures, because the number of quasiparticles at higher temperatures increases. The order of the cooling effect can be estimated as 100 mK (see Fig. S5 in the Supplemental Material [25]), which is comparable to a previous report on a normal-metal–insulator–superconductor tunnel junction [33]. We note that the $0-\pi$ transition of the junction [37] and magnetic impurities [38] in the NW are excluded by the no gate dependence in Fig. 2 and the hysteresis in Fig. 4. Furthermore, the observed hysteresis exclude the topological transition in the proximitized region [23].

Our results reveal that the enhancement of the switching current by an out-of-plane magnetic field is nontopological. However, to realize topological qubits using MFs [39,40], it is important to reduce the quasiparticle density to protect the information of the qubits from quasiparticle poisoning. Even with a higher magnetic field, if the material is a type-II superconductor or thin film in which vortices can penetrate, the device can be designed to trap quasiparticles effectively so that the system of interest is cooled. The effectiveness of quasiparticle trapping is known to depend strongly on device structure [29], and therefore further studies for the optimal design for cooling will be necessary. This Letter shows that quasiparticles in superconducting devices can be reduced by quasiparticle trapping under a finite perpendicular magnetic field, which provides important insights for the design of topological qubit devices in the near future.

Methods.—The InAs NW had a diameter of approximately 80 nm and was grown on an InAs(111)B substrate by chemical beam epitaxy [41]. A Josephson junction was fabricated on the NW after transferring it onto a 280-nm-thick SiO₂ substrate by standard dry transfer technique with cotton buds. Ti/Au markers were fabricated on the substrate in advance, so that we can determine the positions of randomly spread NWs. We made a polymethyl methacrylate pattern for the contact areas using electron beam lithography and performed surface treatment using a (NH₄)₂S_x solution to remove the native surface oxidized layer. Then, the superconducting electrodes were fabricated by depositing Ti/Au

(1 nm/60 nm) and liftoff. The top gate was fabricated by the growth of 20-nm-thick Al₂O₃ by atomic layer deposition, followed by depositing gate electrodes of Ti/Au (50 nm/150 nm) [22,24,41–43].

Measurement setup.—All measurements were made in a dilution fridge with a standard quasi-four-terminal method. The base temperature of the thermal bus was about 35 mK. The conductance was measured with lock-in amplifiers with an excitation voltage of 10 μ V. For the SC measurements, DC voltages across the device were measured with a constant current bias.

For the magnetic-field-dependent measurements, we swept the field at a rate of 0.1 T/min and then waited 15 s before a sweep of bias current.

We thank Prof. S. Jeppesen for the material growth and thank Dr. Shuji Nakamura in AIST for fruitful discussion about thermalization. This work was partially supported by a Grant-in-Aid for Scientific Research (S) (Grant No. JP19H05610), JST PRESTO (Grant No. JPMJPR18L8), Advanced Technology Institute Research Grants, Ozawa-Yoshikawa Memorial Electronics Research Foundation, the Ministry of Science and Technology of China (MOST) through the National Key Research and Development Program of China (Grants No. 2016YFA0300601 and No. 2017YFA0303304) and the National Natural Science Foundation of China (Grants No. 92165208, No. 11874071, No. 91221202, and No. 91421303). K. U. and S. M. designed the device. Y. S., K. U., Y. T., H. K., S. M., and S. T. joined discussions, and their previous results inspired the design. K. U. followed their fabrication process; K. L., L. S., and H. Q. X. provided the nanowires used in the experiment. Y. S. performed experiments with input from K. U., S. M. and S. T.; Y. S. and K. U. wrote the manuscript, with input from all authors. S. M. and S. T. initiated the project.

Y. S. and K. U. contributed equally to this work.

*yosuke.sato@riken.jp

†kento.ueda@riken.jp

‡hqxu@pku.edu.cn

§sodashige.matsuo@riken.jp

||tarucha@riken.jp

- [1] J. Alicea, *Rep. Prog. Phys.* **75**, 076501 (2012).
- [2] Y. Oreg, G. Refael, and F. von Oppen, *Phys. Rev. Lett.* **105**, 177002 (2010).
- [3] S. D. Sarma, M. Freedman, and C. Nayak, *Phys. Today* **59**, No. 7, 32 (2006).
- [4] M. Leijnse and K. Flensberg, *Semicond. Sci. Technol.* **27**, 124003 (2012).
- [5] V. Mourik, K. Zuo, S. M. Frolov, S. Plissard, E. P. Bakkers, and L. P. Kouwenhoven, *Science* **336**, 1003 (2012).
- [6] A. Das, Y. Ronen, Y. Most, Y. Oreg, M. Heiblum, and H. Shtrikman, *Nat. Phys.* **8**, 887 (2012).

- [7] M. Deng, C. Yu, G. Huang, M. Larsson, P. Caroff, and H. Q. Xu, *Nano Lett.* **12**, 6414 (2012).
- [8] M. Deng, C. Yu, G. Huang, M. Larsson, P. Caroff, and H. Q. Xu, *Sci. Rep.* **4**, 7261 (2014).
- [9] S. M. Albrecht, A. P. Higginbotham, M. Madsen, F. Kuemmeth, T. S. Jespersen, J. Nygård, P. Krogstrup, and C. Marcus, *Nature (London)* **531**, 206 (2016).
- [10] L. P. Rokhinson, X. Liu, and J. K. Furdyna, *Nat. Phys.* **8**, 795 (2012).
- [11] D. Laroche, D. Bouman, D. J. van Woerkom, A. Proutski, C. Murthy, D. I. Pikulin, C. Nayak, R. J. van Gulik, J. Nygård, P. Krogstrup, L. P. Kouwenhoven, and A. Geresdi, *Nat. Commun.* **10**, 245 (2019).
- [12] J. Tiira, E. Strambini, M. Amado, S. Roddaro, P. San-Jose, R. Aguado, F. S. Bergeret, D. Ercolani, L. Sorba, and F. Giazotto, *Nat. Commun.* **8**, 14984 (2017).
- [13] C.-X. Liu, J. D. Sau, and S. Das Sarma, *Phys. Rev. B* **97**, 214502 (2018).
- [14] C. Reeg, O. Dmytruk, D. Chevallier, D. Loss, and J. Klinovaja, *Phys. Rev. B* **98**, 245407 (2018).
- [15] E. Prada, P. San-Jose, M. W. de Moor, A. Geresdi, E. J. Lee, J. Klinovaja, D. Loss, J. Nygård, R. Aguado, and L. P. Kouwenhoven, *Nat. Rev. Phys.* **2**, 575 (2020).
- [16] P. Yu, J. Chen, M. Gomanko, G. Badawy, E. P. A. M. Bakkers, K. Zuo, V. Mourik, and S. M. Frolov, *Nat. Phys.* **17**, 482 (2021).
- [17] M. Valentini, F. Peñaranda, A. Hofmann, M. Brauns, R. Hauschild, P. Krogstrup, P. San-Jose, E. Prada, R. Aguado, and G. Katsaros, *Science* **373**, 82 (2021).
- [18] D. I. Pikulin, J. Dahlhaus, M. Wimmer, H. Schomerus, and C. Beenakker, *New J. Phys.* **14**, 125011 (2012).
- [19] M. C. Dartiaillh, J. J. Cuozzo, B. H. Elfeky, W. Mayer, J. Yuan, K. S. Wickramasinghe, E. Rossi, and J. Shabani, *Nat. Commun.* **12**, 78 (2021).
- [20] P.-M. Billangeon, F. Pierre, H. Bouchiat, and R. Deblock, *Phys. Rev. Lett.* **98**, 216802 (2007).
- [21] F. Domínguez, F. Hassler, and G. Platero, *Phys. Rev. B* **86**, 140503 (2012).
- [22] H. Kamata, R. S. Deacon, S. Matsuo, K. Li, S. Jeppesen, L. Samuelson, H. Q. Xu, K. Ishibashi, and S. Tarucha, *Phys. Rev. B* **98**, 041302(R) (2018).
- [23] P. San-Jose, E. Prada, and R. Aguado, *Phys. Rev. Lett.* **112**, 137001 (2014).
- [24] K. Ueda, S. Matsuo, H. Kamata, Y. Sato, Y. Takeshige, K. Li, L. Samuelson, H. Q. Xu, and S. Tarucha, *Phys. Rev. Research* **2**, 033435 (2020).
- [25] See Supplemental Material at <http://link.aps.org/supplemental/10.1103/PhysRevLett.128.207001> for further data to characterize the device, which includes Ref. [26,27].
- [26] M. Tinkham, *Introduction to Superconductivity* (Dover Publications, 2004).
- [27] J. M. Lu, O. Zheliuk, I. Leermakers, N. F. Q. Yuan, U. Zeitler, K. T. Law, and J. T. Ye, *Science* **350**, 1353 (2015).
- [28] A. Murani, S. Sengupta, A. Kasumov, R. Deblock, C. Celle, J.-P. Simonato, H. Bouchiat, and S. Guéron, *Phys. Rev. B* **102**, 214506 (2020).
- [29] J. P. Pekola, O. P. Saira, V. F. Maisi, A. Kemppinen, M. Möttönen, Y. A. Pashkin, and D. V. Averin, *Rev. Mod. Phys.* **85**, 1421 (2013).
- [30] M. Taupin, I. M. Khaymovich, M. Meschke, A. S. Mel'nikov, and J. P. Pekola, *Nat. Commun.* **7**, 10977 (2016).
- [31] S. Nakamura, Y. A. Pashkin, M. Taupin, V. F. Maisi, I. M. Khaymovich, A. S. Mel'nikov, J. T. Peltonen, J. P. Pekola, Y. Okazaki, S. Kashiwaya, S. Kawabata, A. S. Vasenko, J.-S. Tsai, and N.-H. Kaneko, *Phys. Rev. Applied* **7**, 054021 (2017).
- [32] C. Song, M. P. DeFeo, K. Yu, and B. L. Plourde, *Appl. Phys. Lett.* **95**, 232501 (2009).
- [33] J. T. Peltonen, J. T. Muhonen, M. Meschke, N. B. Kopnin, and J. P. Pekola, *Phys. Rev. B* **84**, 220502(R) (2011).
- [34] I. Nsanzineza and B. L. T. Plourde, *Phys. Rev. Lett.* **113**, 117002 (2014).
- [35] C. Wang, Y. Y. Gao, I. M. Pop, U. Vool, C. Axline, T. Brecht, R. W. Heeres, L. Frunzio, M. H. Devoret, G. Catelani, L. I. Glazman, and R. J. Schoelkopf, *Nat. Commun.* **5**, 5836 (2014).
- [36] V. Ambegaokar and B. I. Halperin, *Phys. Rev. Lett.* **22**, 1364 (1969).
- [37] T. Yokoyama, M. Eto, and Y. V. Nazarov, *Phys. Rev. B* **89**, 195407 (2014).
- [38] A. Rogachev, T.-C. Wei, D. Pekker, A. T. Bollinger, P. M. Goldbart, and A. Bezryadin, *Phys. Rev. Lett.* **97**, 137001 (2006).
- [39] D. A. Ivanov, *Phys. Rev. Lett.* **86**, 268 (2001).
- [40] D. Aasen, M. Hell, R. V. Mishmash, A. Higginbotham, J. Danon, M. Leijnse, T. S. Jespersen, J. A. Folk, C. M. Marcus, K. Flensberg, and J. Alicea, *Phys. Rev. X* **6**, 031016 (2016).
- [41] S. Baba, S. Matsuo, H. Kamata, R. Deacon, A. Oiwa, K. Li, S. Jeppesen, L. Samuelson, H. Q. Xu, and S. Tarucha, *Appl. Phys. Lett.* **111**, 233513 (2017).
- [42] S. Baba, C. Jünger, S. Matsuo, A. Baumgartner, Y. Sato, H. Kamata, K. Li, S. Jeppesen, L. Samuelson, H. Q. Xu *et al.*, *New J. Phys.* **20**, 063021 (2018).
- [43] K. Ueda, S. Matsuo, H. Kamata, S. Baba, Y. Sato, Y. Takeshige, K. Li, S. Jeppesen, L. Samuelson, H. Q. Xu, and S. Tarucha, *Sci. Adv.* **5**, eaaw2194 (2019).